O$_2$ electrocatalysis in acid media on iron naphthalocyanine impregnations

Effect of nitric acid treatment on different carbon black supports

F. Coowar, O. Contamin, M. Savy and G. Scarbeck

Laboratoire d'Electrochimie Interfaciale du CNRS, 1, Place Aristide Briand, F92195 Meudon Cédex (France)

D. van den Ham

Twente University, 7500 AE Enschede (The Netherlands)

J. Riga and J.J. Verbist

Facultés N.D. de la Paix, 61, rue de Bruxelles, B 5000 Namur (Belgique)

(Received 13 June 1989; in revised form 7 September 1989)

ABSTRACT

O$_2$ electrocatalysis on (2,3)FeNPc impregnations on different carbon blacks was investigated in H$_2$SO$_4$ medium. The effect of nitric acid treatment on the carbon black support is to enhance both the activity and stability of the catalyst. Moreover, as seen by XPS, the dissolution of iron is impeded by this oxidation treatment which, however, does not increase the density of active sites with the BET surface area. From the data presented, a redox mechanism can hardly be invoked, in contrast to the situation for FeNPc impregnations on active charcoals.

INTRODUCTION

Among the various modes of chemical energy conversion into electricity there is still a sustained interest in fuel cells operating at temperatures below 100°C [1]. A major bottleneck in their development lies in the utilization of Pt catalysts; N$_4$ chelates may offer a substitute for O$_2$ reduction in acidic electrolytes [2]. The major problem here is how to optimize the carbon black or active charcoal support structure.

Iron naphthalocyanine (FeNPc) impregnated on exCH$_4$ carbon black was found to be unstable in sulphuric acid [3], but in the same solutions when synthesized on

Norit BrX active charcoal, an increase in activity was observed [4] despite considerable demetallation.

As this active charcoal contains basic groups [5] on its surface and possesses a large amount of iron, it is difficult to shed light on the role of the FeNPc/substrate interface bonding on the O_2 electrochemical process. In ref. 3, FeNPc was prepared from dicyanonaphthalene "(1,2)DCN" following the route described in ref. 6. However, this method gives rise to a mixture of 4 isomers which can hardly be separated.

Recently, a method of FeNPc synthesis yielding a single isomer has been reported starting from "(2,3)DCN" [7]. The most common carbon support material for O_2 electrocatalyst Pt is a Cabot furnace black called Vulcan XC 72 [8]. It can be treated with nitric acid in order to introduce acidic groups, such as carboxylic functional groups, on its surface [9].

It has been shown in a number of papers that the character of the surface functional groups influences the electrocatalytic properties of active carbons [10]. The aim of this paper is to investigate, for the case of carbon blacks, the effect of acid treatment of the (2,3)FeNPc impregnation supports on their properties for O_2 electrocatalysis in sulphuric acid medium. In order to show the influence of the BET surface area, two carbon blacks were selected, namely Vulcan XC 72 and Degussa XE 2.

EXPERIMENTAL

Material synthesis and characterizations

Dicyanonaphthalene "(2,3)DCN" was prepared according to a method given in the literature [11]. FeNPc was then synthesized by heating "(2,3)DCN" and Fe acetylacetonate (FeAcAc) for 5–6 h in the presence of ammonium molybdate as catalyst at 260–270 °C in a sealed tube [7]. In this synthesis mode, the molar ratio was 4 : 1, i.e. 4 mol "(2,3)DCN" per mol FeAcAc.

Impregnations were obtained by adding to the reactant mixture in the 4 : 1 molar ratio, the following carbon black powders: Vulcan XC 72, treated Vulcan XC 72 and treated Degussa XE 2. The amount of iron determined by atomic absorption was found to oscillate between 0.6 and 0.7% W/W. The powder preparation without carbon black was dissolved in pyridine and characterized using UV–Vis spectroscopy. All these measurements were conducted using a Cary model 17 spectrophotometer with a 10 mm quartz cuvette at a concentration of 10^{-5} mol dm^{-3}. Figures 1a and b depict the absorbance spectra under N_2 and O_2, respectively.

Compared to FeNPc resulting from "(1,2)DCN", a shift to longer wavelengths of 80 nm in favour of (2,3)FeNPc can be observed for the maximum Q band absorption peak. This finding is in good agreement with literature reports [12]. It may be noted that for the Q band the absorbance intensity is higher under O_2 than under N_2. Therefore we conjecture an interaction with dioxygen.

In the impregnation case a small quantity of FeNPc solution was eluted with pyridine and characterized as mentioned above. The same spectra were obtained.
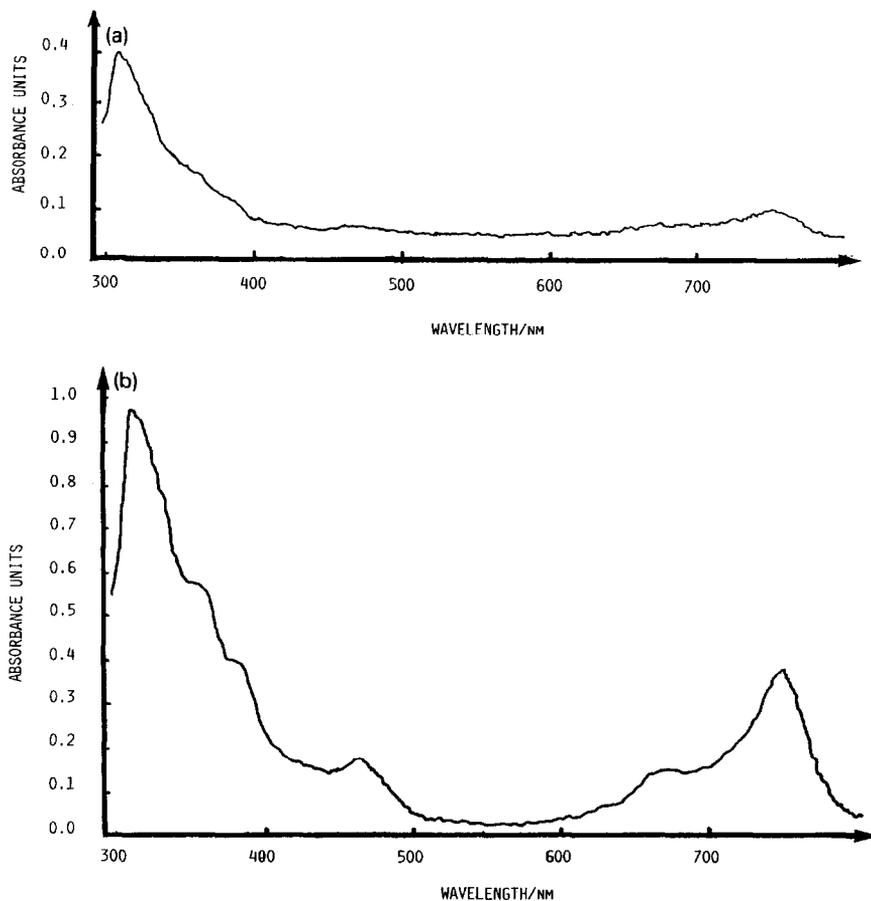
Fig. 1. (a) Absorption spectrum under N_2 of FeNPc (2,3) dissolved in pyridine. (b) Same as (a), but under O_2.

Further investigations were pursued using elemental analysis on the non-supported powder. The results are presented in Table 1. As for C, H and N, we can presume that the naphthalocyanine skeleton is formed. The slight deficiency in iron

TABLE 1

Elemental analysis

	w/w %			
	C	H	N	Fe
Found	73.88	3.15	14.55	6.29
Expected	75.0	3.10	14.6	7.3

indicates the probable presence of H_2NPc, which is known to be inactive for O_2 reduction.

XPS characterizations were also carried out and are reported in the Discussion. The XPS analyses were performed on an HP 5950 A spectrometer using monochromatized Al K_α 1.2 radiation, $h\nu = 1486.6$ eV. For more experimental details, see ref. 4.

Carbon black treatment

The carbon surface treatment consisted in exposing the carbon black to 7 mol/l HNO_3 acid for 5 h at 90 °C. The aim of this treatment was to introduce surface acidic groups such as the carboxylic functional group [9]. After this chemical treatment, Degussa XE2 and Vulcan XC72 were investigated further by FT-IR transmission techniques. Untreated active charcoal (Norit BrX) was taken as a reference. The apparatus used was a Nicolet 5 SXC with a resolution power of 4 cm^{-1}.

Surface group absorption peaks were only visible on the large BET surface area samples Norit BrX and Degussa XE2 (Figs. 2a and b, respectively). As Vulcan XC72 presents a lower BET surface area, 250 m^2/g, compared to 1800 m^2/g for Norit and 1000 m^2/g for Degusssa XE2, its FT-IR spectrum was hardly interpretable.

According to refs. 9 and 13, in the Norit BrX case the two peaks located near 2910 cm^{-1} can be assigned to CH bonds, the peak at 1730 cm^{-1} results from a carboxyl group and the band near 1570 cm^{-1} from neutralized carboxylic groups. On Degusssa XE2 the peak intensities at 1730 cm^{-1} and 1540 cm^{-1} are higher than on Norit BrX, a result which can be interpreted according to the same refs. 9 and 13 as being due to more acidic carboxylic groups. Due to the surface chemical structure one can assume the same conclusions in the Vulcan case.

Electrochemical measurements

A classical cell with three electrodes was used with a RHE as reference. A large Pt counter electrode was fixed at the bottom of the cell. The electrochemical measurements were conducted using a rotating disc electrode (RDE) and voltammetry. The measurements were obtained by a potentiostat monitored by a Fabelle ST1 generator. Data were recorded using a Reptec PC equipped with a DT 2814 card. The impregnated catalyst was inserted in a hollow cavity of 0.4 mm depth in a disc. Then this electrode was tested using ferri/ferrocyanide solutions; this yielded a Levich plot (i_L versus $f^{1/2}$, where i_L is the diffusing limiting current, and f the rotation frequency).

In all cases, before applying the catalyst a gold lacquer (Degussa M 8001) was brushed over the cavity surface in order to minimize the ohmic drop between the Au support and the grains [4]. All the experiments were conducted using an electrode of apparent surface area $A = 0.125$ cm^2.

All the experiments were carried out in solutions prepared from suprapur Merck H_2SO_4 diluted with Millipore super Q water. The solutions investigated were 0.25 M H_2SO_4.
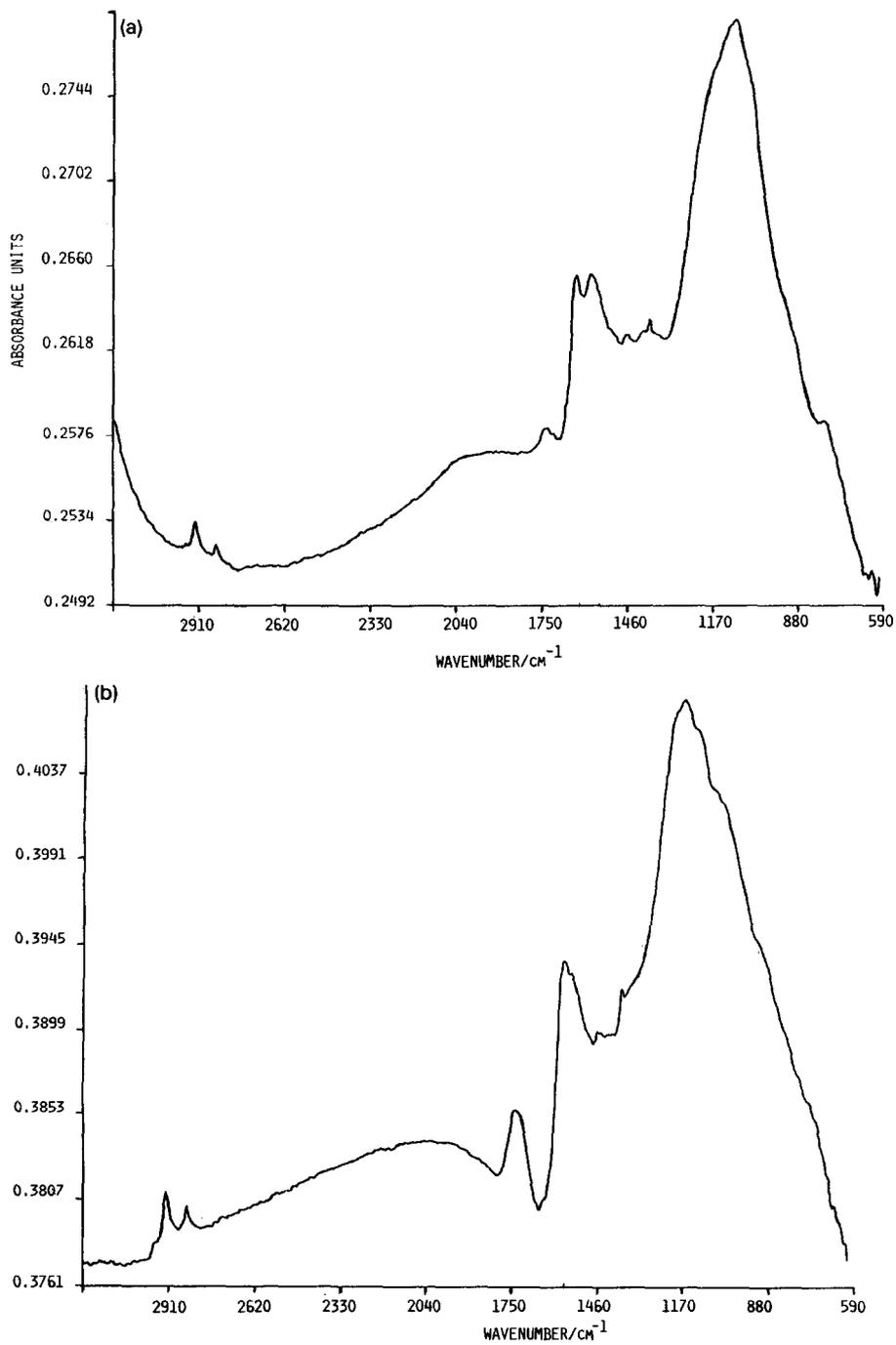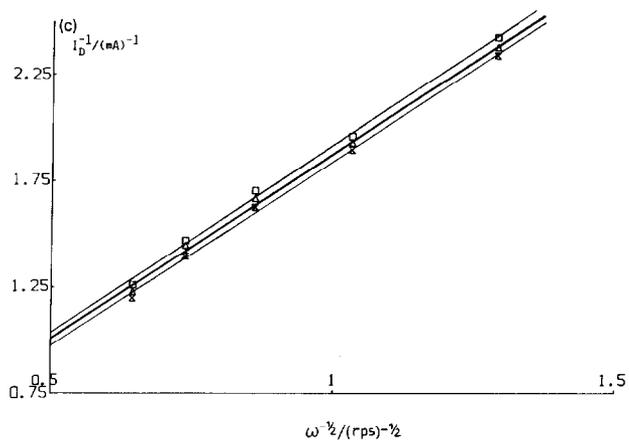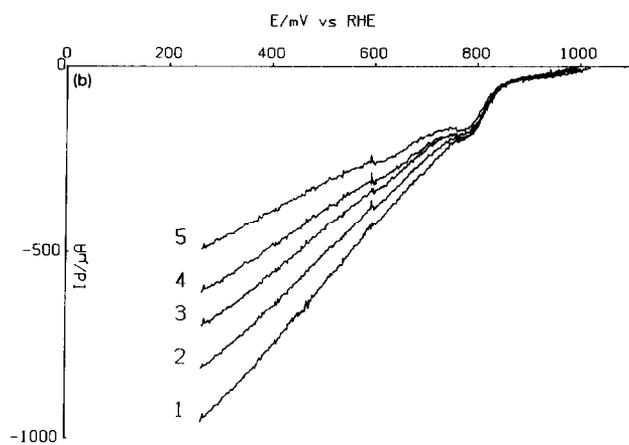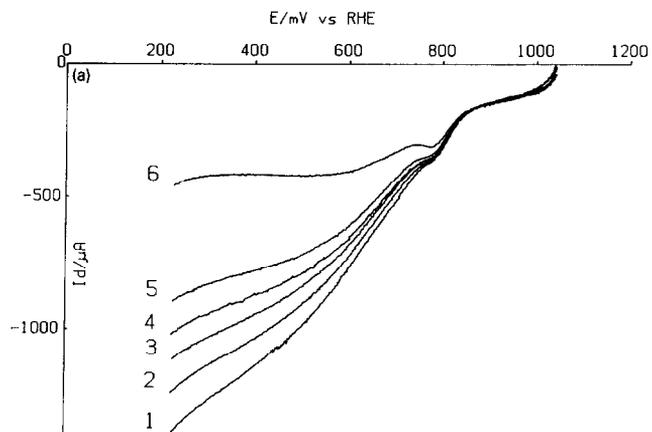
Fig. 2. FTIR spectra on non-impregnated Norit BRX (a) and Degussa XE2 (b).

RESULTS AND DISCUSSION

Figure 3a depicts the $i-E$ curves obtained for impregnated FeNPc on untreated Vulcan XC 72 at different rotation frequencies. No limiting current can be observed. For obtaining the true oxygen reduction current one can subtract from each curve the residual current measured under N_2. Figure 3b shows the curves resulting from Fig. 3a after subtraction of the curve under N_2. The curves under N_2 were obtained after polarizing the electrodes at 600 mV/RHE in order to get rid of O_2 impurities. The current density was found to be zero. Then the curves were recorded.

To determine n, the number of electrons involved in the overall reaction per O_2 molecule, we assumed first order kinetics with respect to dissolved O_2. Under such conditions the observed currents in a rotating disc study are related to the rotation rate [14] by the equation:

$$1/i = 1/i_k + 1/B\omega^{1/2} \tag{1}$$

where i_k is the kinetic current and i_D the corresponding diffusion current equal to $B\omega^{1/2}$.

$$B = 0.62 nFD^{2/3} \nu^{-1/6} c(O_2) \tag{2}$$

Here, D is the O_2 diffusion coefficient, ν the kinematic viscosity, $c(O_2)$ the O_2 concentration in solution and $\omega = 2\pi f$, where f is the rotation rate.

The plot of $1/i$ versus $\omega^{-1/2}$ at different potentials assuming a uniform current distribution [15] should yield parallel straight lines at different potentials. The linearity and parallelism of Fig. 3c confirm first order kinetics with respect to dissolved oxygen and the validity of eqn. (1). These parallel straight lines were obtained at potentials of 350, 370 and 380 mV/RHE, respectively. The correlation coefficient R is equal to 0.998.

The fact that these lines do not pass through the origin indicates the occurrence of a kinetic limitation. This is attributed by Durand and Anson [16] to a rate determining chemical reaction between dioxygen and the catalyst. According to ref. 17, current or kinetic saturation occurs as the time needed by a dioxygen molecule to traverse through the convective diffusion layer becomes comparable to the time required to diffuse across the surface to an active site. Surface diffusion can explain the kinetic limitation. Both explanations (a rate determining chemical step or surface diffusion) are equally probable; the second explanation has, however, the advantage that it does not require the introduction of a rate determining step. In this case the time of O_2 diffusion across the active sites is greater than the time required for an O_2 molecule to cross the diffusion layer.

Fig. 3. (a) $i-E$ curves obtained on impregnated FeNPc on untreated Vulcan XC 72 at different rotation rates, f. Scanning velocity 1.5 mV/s. f/rps: (1) 64; (2) 49; (3) 36; (4) 25; (5) 16; (6) 0. (b) Curves resulting from (a) after subtraction of the curve under N_2. (c) Koutecky–Levich plots ($1/i$ versus $\omega^{-1/2}$) at different potentials; curves resulting from (b). (X) 350; (△) 370; (□) 380 mV.

TABLE 2

The overall number of electrons exchanged, n_{exp}; the reaction order with respect to dissolved oxygen, m; and the B values calculated from eqn. (2), at different potentials

E/mV	n_{exp}	m	B_{exp} (rate)/ mA (rpm)$^{-1/2}$	B (calculated)/ mA (rpm)$^{-1/2}$
380	3.7	1.2	0.42	0.44
370	3.6	1.1	0.40	0.44

It has been shown that plots of this type are relatively insensitive to deviations from first order kinetics [18]. Consequently, the reaction order was checked by calculation using eqn. (3) provided in ref. 19.

$$\log i_d = \log i_k + m \log \left(1 - i_d/i_{dl}\right) \tag{3}$$

where i_d and i_{dl} are the disc and diffusion limiting currents, respectively. In Table 2 the results are gathered for the number of overall exchange electrons n, the reaction order m and B being defined above. From this table it turns out that the reaction order with respect to dissolved oxygen is 1 and the number of exchanged electrons is close to 4. The B values were obtained from ref. 20.

Figures 4a and b present the voltammograms obtained on stationary electrodes at different scanning velocities after several cycles under N_2 and O_2, respectively. The slight hump visible under O_2 around 0.78 V/RHE during the first scan (Fig. 3a, curve 6) vanishes almost completely after recycling. If one examines Fig. 4b carefully, a slight hump can also be detected on the positive scans. In contrast to our previous results, reported in refs. 3 and 4, a redox mechanism can hardly be invoked on impregnated FeNPc on Norit BrX. In the range of potentials corresponding to O_2 reduction a slight peak can be observed, whereas under the same conditions no peak can be detected under N_2. The hump located at around 780 mV/RHE (Fig. 3a, curve 6) under O_2 can, according to these references, be assigned to an O_2 adduct reduction of the μ-oxo or μ-peroxo type. The existence of the O_2 adduct can be confirmed from Fig. 1b, which characterizes the optical absorption spectrum in pyridine of dissolved FeNPc under O_2. The peak located at 670 nm is higher than the one observed under N_2. In refs. 21–23, the formation of dioxygen bridge dimers has been proposed. More recently, these adducts have been reported in acid media [24,25]. Figure 3a shows i–E curves obtained on impregnated FeNPc on treated Vulcan at different rotation rates.

In contrast to the preceding case, a pseudo-limiting current can be defined. Figure 5b results from Fig. 5a after subtraction from each curve of the current measured under N_2 and defined as mentioned above. In this case results can be analyzed by plotting i_L versus $f^{1/2}$ (Fig. 5c). From this curve the linear slope turns out to be 123 μA (rps)$^{-1/2}$, which is close to the theoretically calculated value for the 4-electron reduction process (125 μA (rps)$^{-1/2}$) from ref. 20. The linear plot obtained has a correlation coefficient of $R = 0.985$.
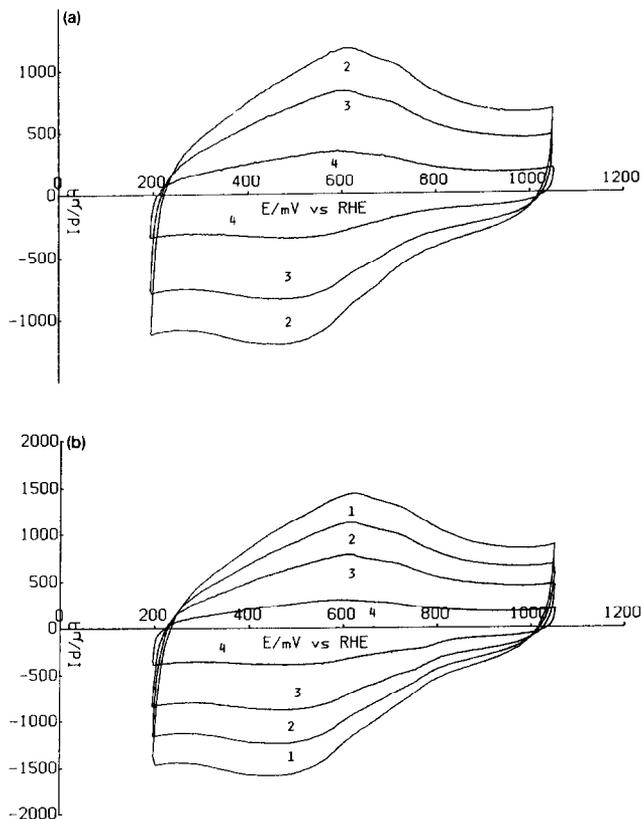
Fig. 4. (a) Voltammograms obtained on a stationary electrode at different scanning velocities for impregnated FeNPc on untreated Vulcan under N_2. Scan rate/mV s^{-1}: (1) 8; (2) 6; (3) 4; (4) 1.5. (b) Same as (a) under O_2.

The fact that this line does not pass through the origin indicates the probable participation of internal sites. However, at 64 rps their contribution is relatively small compared to that of the external sites. The internal sites can be defined as O_2 reservoirs supplying an additional O_2 reduction current to the one due to dissolved oxygen in the electrolyte.

Figures 6a and b show the voltammograms obtained on stationary electrodes at different scanning velocities identical to those displayed in Figs. 4a and b. The same conditions were used as in Figs. 4a and b. As in the previous case, O_2 reduction cannot be associated with a redox mechanism. Moreover, no oxygen adduct can be detected.

In contrast to the previous case, the rate determining step (in the range of potentials where a limiting current is observed) consists in the diffusion of O_2 in the convective diffusion layer. The diffusion of O_2 across the active sites is rapid compared to the diffusion of O_2 in the solution. It is possible to plot $\log(i/i_L - i)$
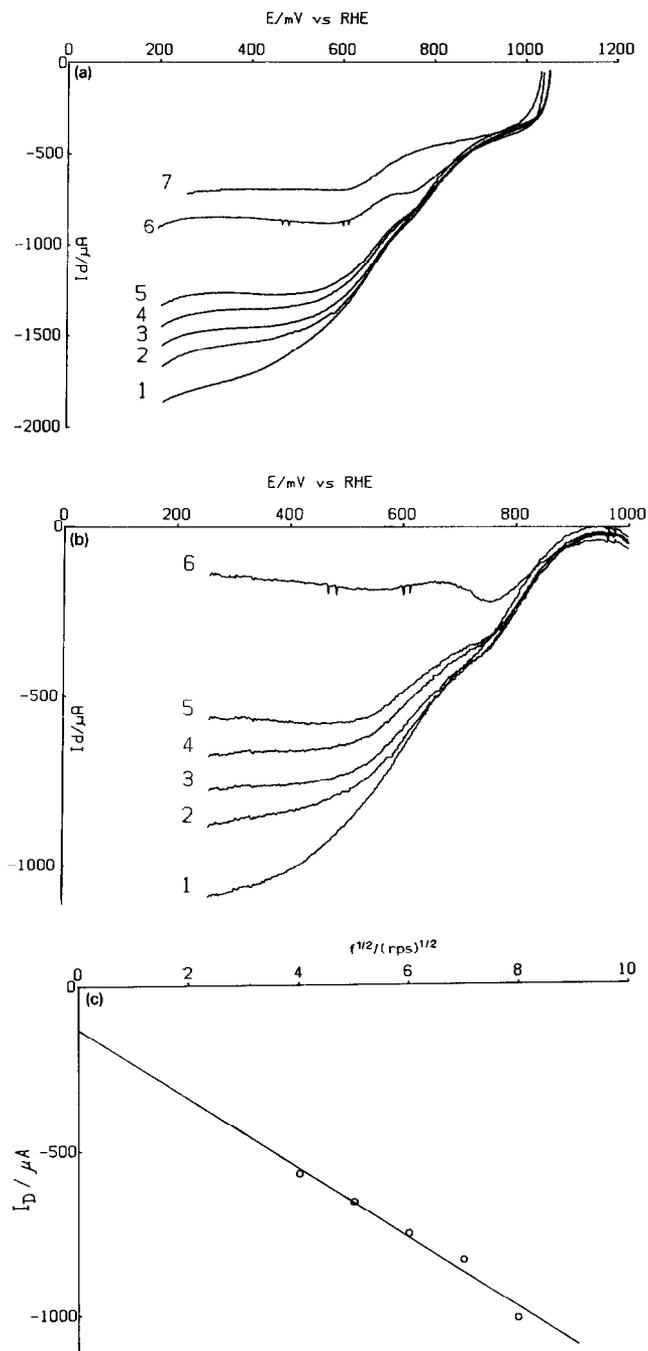
Fig. 5. (a) $i-E$ curves obtained for impregnated FeNPc on treated Vulcan at different rotation rates. Same parameters as in Fig. 3a (curve 7: under N_2). (b) Same as (a) after subtraction of the current measured under N_2. (c) Levich plots resulting from the curves presented in (b).
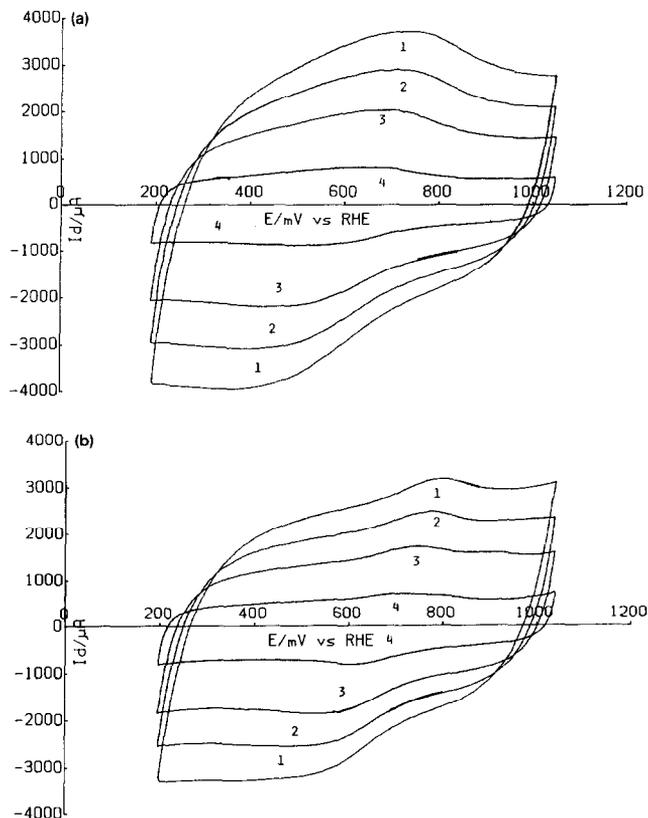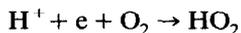
Fig. 6. (a) Voltammograms obtained on a stationary electrode at different scanning velocities for impregnated FeNPc on treated Vulcan under N_2. Same conditions as in Fig. 4a. (b) Same as (a) but under O_2.

versus E. A linear slope is obtained equal to 116 mV per decade, characteristic of a one-electron transfer in the rds associated with a diffusion process of the type:

$$H^+ + e + O_2 \rightarrow HO_2$$

followed by a fast reduction of HO_2 into water.

Figure 7a presents $i-E$ curves obtained for impregnated FeNPc on treated Degusssa XE2 at different rotation rates as defined in Fig. 3a. At low overvoltages an O_2 reduction current can be observed. In Fig. 7b the same curves are shown as in Fig. 7a after subtraction of the current under N_2.

A hump in the current is clearly visible at $E = 760$ mV/RHE. As no limiting current can be detected, a Koutecky–Levich plot can be obtained (Fig. 7c). From this figure it can be deduced that, since parallel straight lines are obtained at different potentials (310, 340 and 380 mV/RHE) with a reciprocal of the slope yielding $n = 3.6$, a four-electron process is involved. These parallel straight lines at
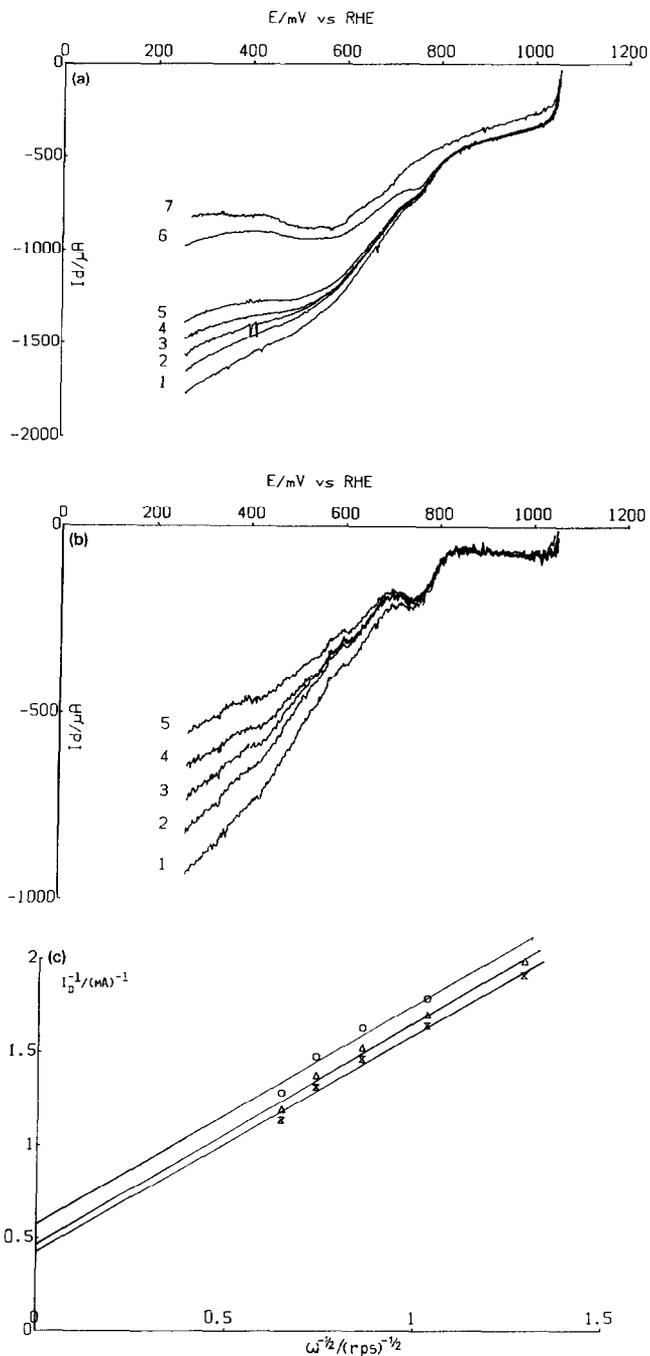
E/mV vs RHE

(a)

7
6
5
4
3
2
1

I/μA

E/mV vs RHE

(b)

5
4
3
2
1

I/μA

(c)

$I_D^{-1}/(mA)^{-1}$

$\omega^{-1/2}/(rps)^{-1/2}$

Fig. 7. (a) $i-E$ curves obtained for impregnated FeNPc on treated Degussa XE2 at different rotation rates. Same conditions as in Fig. 3a (curve 7: under N_2). (b) Same as (a), after subtraction. (c) Koutecky–Levich plots ($1/i$ versus $\omega^{-1/2}$) at different potentials (curves resulting from (b)). ($\times$) 310; ($\triangle$) 340; ($\bigcirc$) 380 mV.

different potentials were obtained with a correlation coefficient of 0.99. As they do not pass through the origin, the same conclusions can be drawn as above in the case of FeNPc on untreated Vulcan. The rate determining step (rds) consists in a chemical reaction between dioxygen and the catalyst or O_2 diffusion across the active sites.

The main difference in the O_2 reduction kinetics between FeNPc impregnations on treated Vulcan and treated Degussa lies in the rds. Whereas in the impregnation on treated Vulcan the rds is governed by O_2 diffusion in the electrolyte diffusion layer thickness, in the two other cases the rds appears to be controlled either by O_2 diffusion across the active superficial sites of the catalyst ($1/i$ proportional to $\omega^{-1/2}$) or to a chemical reaction between dioxygen and the catalyst.

As mentioned above for the two carbon blacks pretreated with HNO_3, the only difference lies in the BET surface area, which was 1000 m^2/g and 256 m^2/g for Degussa XE2 and Vulcan XC 72, respectively. The differences in activity can thus
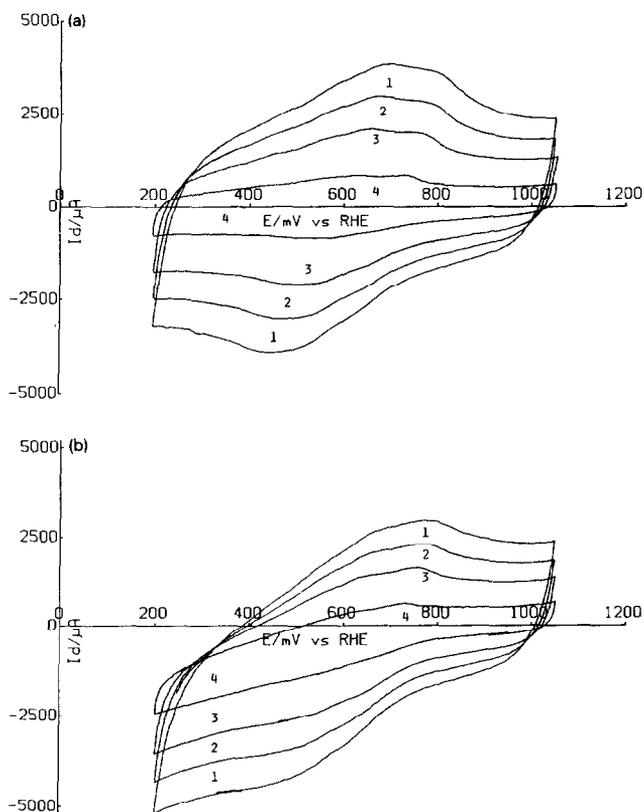

Fig. 8. (a) Voltammograms obtained at a stationary electrode at different scanning velocities for impregnated FeNPc on treated Degussa XE2 under N_2. Same conditions as in Fig. 4a. (b) Same as (a) but under O_2.

be interpreted in terms of the density of active sites, which is higher on treated Vulcan than on treated Degussa XE2.

Our results show the beneficial effect of chemical treatment of carbon black, but in our experimental conditions the BET surface area turns out to play an important role in the active center density.

Figures 8a and b display the voltammograms obtained on impregnated FeNPc on treated Degussa XE2 under N_2 and O_2, respectively, at a stationary electrode. Under N_2, whereas two visible peaks can be detected on the positive scans, only one peak is visible for negative scans at 560 mV/RHE for $v = 1.5$ mV/s. Under O_2, only one peak is visible on the positive scan. From Fig. 8b, O_2 reduction begins at 760 mV/RHE, which lies above the potentials found for the cathodic peak under N_2. Therefore a redox process can hardly be invoked for O_2 reduction.

It should be stressed that, in all the three cases explored, the O_2 reduction mechanism does not appear to be associated with a redox process, in contrast to previous results reported for FeNPc impregnated on other different supports [3,4]. This result emphasizes the role of the support in the kinetics and reaction mechanism.

STABILITY

For the stability experiments the electrodes were prepared according to the following procedure: 0.1 g of impregnated carbon black was added to 0.1 ml of a Soreflon solution at 48 g/l concentration which served as a binding agent (Soreflon is a teflon suspension purchased from Société Française de Matières Colorantes). 3 ml of pure ethanol were also added. The resulting paste was mixed and dried in an oven at 80°C for 10 min after application to the hollow cavity of the disc.

Voltage loads of 600, 700 and 800 mV/RHE were then applied directly to the electrodes (Table 3). Steady currents were obtained after a period which depends upon the applied potential. At 600 mV/RHE they are reached within 20 h and at 800 mV/RHE within 3 days. After one week under a constant voltage load the variations in current density remained below 7%. The rotation frequency was kept

TABLE 3

Stability tests at different potentials for the impregnations investigated

E/mV (RHE)	Steady current/μA		
	Vulcan	Treated Vulcan	Treated Degussa XE2
600	510	800	760
700	153	300	260
800	45	180	35
Tafel slope, E versus $\log(i/i_L - i)$/ mV decade	140	120	80

TABLE 4

C/O ratios on carbon blacks as determined by XPS

	Untreated Vulcan	Treated Vulcan	Treated Degussa XE2
C/O	40	60	20

constant at 64 rps. The differences with the data reported in Figs. 3b, 5b and 7b must be emphasized.

In the Vulcan and treated Vulcan cases (FeNPc impregnated), plots of E versus $\log(i/i_L - i)$ yield a slope of about 120 mV, indicating an initial one-electron transfer as the rds [4,26]. In contrast, for impregnated FeNPc on treated Degusssa XE2, the calculated slope (80 mV per decade) is characteristic of a reaction whose rate is controlled by the catalyst concentration [27]. i_L is the theoretical steady current at 64 rps calculated from data reported in ref. 20, and i is the current obtained after one week's voltage load. In contrast with the figures mentioned above, no hump at around 780 mV/RHE is noticeable.

According to Table 3, the most salient feature lies in the improvement of the electrocatalytic activity in the two treated support cases, and more especially in the treated Vulcan impregnations. The effect of nitric acid treatment consists in an enhancement of the active sites. Similar results were found when the same treatment was applied to pure carbon blacks [9]. A tenfold current density increase was observed at constant voltage for O_2 reduction. These results were interpreted in terms of surface acidic group formation. These surface groups were characterized using FT-IR techniques [13].

To obtain insight into the oxidation effect due to the chemical treatment, XPS investigations were carried out on the carbon support and on the impregnated catalysts. Results are given in Table 4 for carbon blacks. In the three cases one can notice the absence of nitrogen and the existence of an O_{1s} peak centered at 532.5 eV which is characteristic of a weakly bonded oxygen. Comparison of the treated and untreated Vulcan reveals an oxygen loss in the case of treated Vulcan, as one can hardly imagine an increase of the carbon atoms. The specific low rate of C/O in the Degussa XE2 case can easily be explained in terms of its higher BET surface area, oxygen being confined to the surface.

TABLE 5

C/O, C/N and C/Fe ratios in the different FeNPc impregnations

	Untreated Vulcan	Treated Vulcan	Treated Degussa XE2
C/O	25	17	25
C/N	40	52	50
C/Fe	810	420	1050

The XPS results concerning the C/O, C/N and C/Fe ratios after one week's stay in O_2 saturated 0.25 M H_2SO_4 in the case of FeNPc impregnations are gathered in Table 5 for these three different supports. In the three cases mentioned above, the O_{1s} N_{1s} and Fe_{2p} peaks are relatively similar.
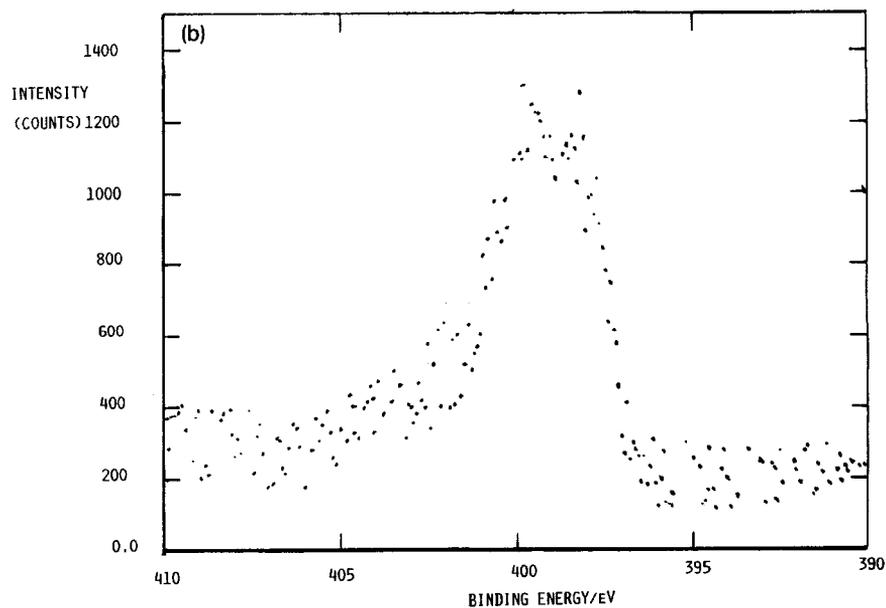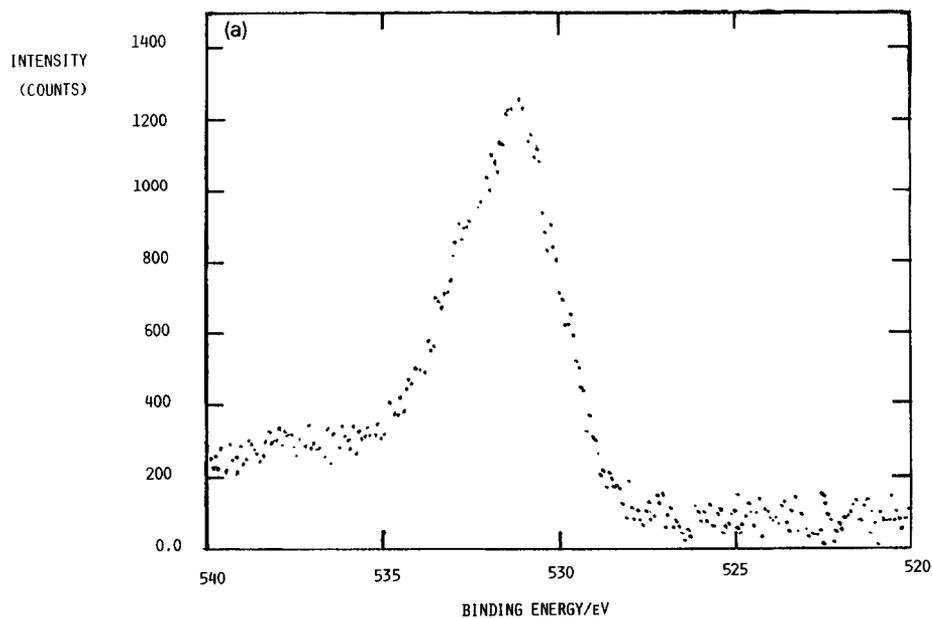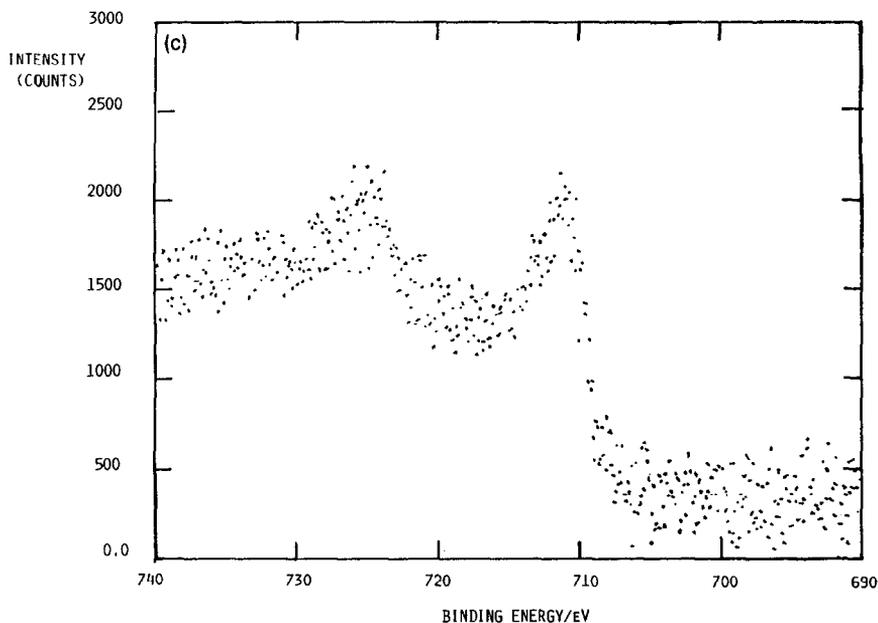
Fig. 9. XPS spectra on impregnated FeNPc samples after a prolonged stay in 0.25 M H_2SO_4 solution under O_2. (a) Typical O_{1s} spectrum. (b) Typical N_{1s} spectrum. (c) Fe_{2p} spectrum for the impregnated treated Vulcan case.

The O_{1s} spectrum is depicted in Fig. 9a. Two peaks are discernible, located at 531.5 and 533 eV. They correspond to strongly and weakly bonded oxygen, respectively. In the untreated impregnated Vulcan case the peak at 533 eV is less marked. A typical N_{1s} spectrum is represented in Fig. 9b. It is characteristic of FeNPc [28] with two peaks located at 398.7 and 400.1 eV. Figure 9c shows the Fe_{2p} spectrum, which is better defined in the treated Vulcan impregnation case. It presents the characteristic of a valency III oxidation state. In contrast to our previous results, reported in ref. 4, concerning FeNPc impregnations on Norit BrX, it has to be pointed out that the Fe_{2p} signal remains much higher. The main difference with the samples which had not been in contact with sulphuric acid lies in the oxidation state of iron, which has a valency of II in this case.

From Table 5 it turns out that the lowest C/Fe ratio is obtained for treated Vulcan impregnations. Comparison with Table 2 shows a correlation between the rds resulting from the Tafel slope and the C/Fe ratio. The lowest Fe content yields a rds involving the catalyst concentration. In addition, between treated and untreated Vulcan the highest Fe/C ratio corresponds to the best catalyst. Thus, the specific role of Fe in the stability and activity of the catalyst for O_2 reduction has to be stressed.

The effect of the nitric acid treatment on Vulcan is to inhibit iron dissolution into the electrolyte. As the N_{1s} peaks remain unchanged for the three samples after prolonged contact with the acid solution, one can assume that nitrogens play a negligible role in the linkage between the FeNPc molecule and the substrate. The same assumptions hold for the oxygens from their O_{1s} spectra. Thus, one can infer a bond between iron and the substrate which is strengthened by the nitric acid treatment. It has to be noted that the enriched iron samples yield a higher weakly bonded oxygen concentration which is involved in the electrocatalysis. The surface acidic groups may hold the iron atom during the FeNPc synthesis, preventing its further dissolution. This finding is in contrast with ref. 5, in which the presence of basic groups on Norit BrX was found to be required to enhance O_2 electrocatalytic activity. In ref. 4, considerable iron losses were found for FeNPc impregnations on this active charcoal. Thus, from our data it seems that surface acidic groups are a prerequisite for long term stability on these impregnated catalysts. Our results support the view developed in ref. 10 that some optimum exists for the ratio between the amount of basic and acid surface groups on carbon blacks for O_2 reduction electrocatalysis. As already mentioned above, the main difference between FeNPc impregnation on Norit BrX and on the investigated carbon blacks resides in the absence in the present case of a redox mechanism. In the RDE experiments and in the stability tests the rds was found to be the formation of HO_2 linked to the central iron. The oxidation state of the iron remains at the same valency, as shown by XPS experiments. In the FeNPc impregnation on Norit BrX the rds was Fe^I/Fe^{II} oxidation.

The enhancement of the activity observed in the present case can be correlated to direct bond formation between iron and the substrate via carboxylic groups and can be interpreted in terms of the back bonding model [29,30] coming from MO theory. The effect of the fifth ligand of the iron is to raise the d_{z^2} orbital, thus enhancing electron donation from the O_2 molecule. Back bonding with antibonding π^* of the O_2 molecule is possible as the d_{xz} or d_{yz} orbitals of Fe^{3+} are filled.

CONCLUSION

Investigations which have been carried out using the RDE, voltammetric techniques and stability tests show the same rds on FeNPc impregnations on carbon black. This rds does not appear to correspond to a redox mechanism, in contrast to FeNPc impregnations on Norit BrX. Moreover, the effect of the treatment on carbon blacks prevents iron dissolution in acid media as long as the BET surface area is not too high.

Especially at low overvoltages (800 mV/RHE) a considerable increase (more than fourfold) in current density can be noted during the stability tests compared to our previous results on FeNPc Norit BrX impregnations.

Under optimal conditions, the iron of the FeNPc molecule seems to be linked to the substrate via carboxylic groups without any deformation of the FeNPc molecule.

This bond confers to the active sites (central iron) electrocatalytic properties which can be interpreted in the light of the back bonding model.

REFERENCES

1 S. Srinivasan, J. Electrochem. Soc., 136 (1989) 41C.
2 R. Franke, D. Ohms and K. Wiesener, J. Electroanal. Chem., 260 (1989) 63.
3 F. Coowar, O. Contamin, M. Savy and G. Scarbeck, J. Electroanal. Chem., 246 (1988) 119.
4 F. Coowar, M. Savy, G. Scarbeck, D. van den Ham, J. Riga and J.J. Verbist, J. Electroanal. Chem., 259 (1989) 241.
5 J.A.R. van Veen and C. Visser, Electrochim. Acta, 24 (1979) 921.
6 E.F. Bradbrook and R.P. Linstead, J. Chem. Soc., (1935) 1744.
7 S. Deger and M. Hanack, Synth. Met., 13 (1986) 319.
8 J. McBreen, H. Olender, S. Srinivasan and K.V. Kordesch, J. Appl. Electrochem., 11 (1981) 787.
9 N. Muira, K. Gonryo, N. Yamazoe and T. Seiyama, Chem. Lett., (1981) 1279.
10 I.A. Kukushkina, G.V. Shteinberg and A.V. Dribinskii, Elektrokhimiya, 21 (1985) 1384 and references therein.
11 E.A. Lukyanets and S.A. Mikhalenko, J. Gen. Chem. USSR, 39 (1969) 2449.
12 E.A. Lukyanets and S.A. Mikhalenko, Zh. Obshch. Khim., 39 (1969) 2129.
13 C. Prado Burguete, A. Linares Solano, F. Rodriguez Reinoso and C. Salinas Martinez de Lecea, J. Catal., 115 (1989) 98.
14 V.G. Levich, Physicochemical Hydrodynamics, Prentice Hall, Englewood Cliffs, NJ, 1962.
15 J. Newman, J. Phys. Chem., 70 (1966) 1327.
16 R.R. Durand and F.C. Anson, J. Electroanal. Chem., 134 (1982) 273.
17 J.D.E. McIntyre and W.F. Peck, Jr., Proc. Electrochem. Soc. (The Chemistry and Physics of Electrocatalysis), The Electrochemical Society, Princeton, NJ, D 84 (1984) 102.
18 J.T.Yu. Tryk and E. Yeager, Electrochem. Soc. Meeting, Montreal, May 1982, The Electrochemical Society, Princeton, NJ, Ext. Abstr., 82-1, p. 674.
19 B.B. Damaskin and O.A. Petrii, Introduction to Electrochemical Kinetics, Vyshaya Schkola, Moscow, 1983, p. 172.
20 K.E. Gubbins and R.D. Walker, J. Electrochem. Soc., 134 (1965) 469.
21 D.M. Wagnerova, E. Schwertnerova and J. Veprek Siska, Collect. Czech. Chem. Commun., 39 (1974) 1980.
22 L.C. Giruen and R.J. Blagrove, Aust. J. Chem., 26 (1973) 319.
23 J.H. Schutten, Ph.D. Thesis, Eindhoven University of Technology, 1981.
24 B. Simic Glavaski, S. Zecevic and E. Yeager, J. Electroanal. Chem., 150 (1983) 469.
25 D. van den Ham, C. Hinnen, G. Magner and M. Savy, J. Phys. Chem., 91 (1987) 4743.
26 J. Zagal, R.K. Sen and E. Yeager, J. Electroanal. Chem., 83 (1977) 207.
27 J.P. Collman, P. Denisevich, Y. Kanai, M. Marrocco, C. Koval and F.C. Anson, J. Am. Chem. Soc., 102 (1980) 6027.
28 J. Riga, M. Savy, J.J. Verbist, J.E. Guerchais and J. Sala Pala, J. Chem. Soc. Faraday Trans. 1, 78 (1982) 2773.
29 H. Alt, H. Binder and G. Sanstede, J. Catal., 28 (1973) 8.
30 H. Jahnke, M. Schonborn and G. Zimmerman, Top. Curr. Chem., 61 (1976) 133.